

Regiospecific Intramolecular O-Demethylation of the Ligand by Action of Molecular Dioxygen on a Ferrous Complex: Versatile Coordination Chemistry of Dioxygen in FeCl₂ Complexes with (2,3-Dimethoxyphenyl) α -Substituted Tripods in the tris(2-Pyridylmethyl)amine Series

Laila Benhamou,^{†,‡} Ahmed Machkour,^{†,‡} Olaf Rotthaus,[†] Mohammed Lachkar,[‡] Richard Welter,[§] and Dominique Mandon*[†]

[†]Laboratoire de Chimie Biomimétique des Métaux de Transition, Institut de Chimie, UMR CNRS no. 7177, Université Louis Pasteur, 4 rue Blaise Pascal, B.P. 1032, F-67070 Strasbourg cedex, France, [‡]Laboratoire d'Ingénierie des Matériaux Organométalliques et Moléculaires, Université Sidi Mohamed Ben Abdellah, Faculté des Sciences, BP 1796 (Atlas), 30000 Fez, Morocco and [§]Laboratoire DECOMET, Institut de Chimie, UMR CNRS no. 7177, Université Louis Pasteur, 4 rue Blaise Pascal, B.P. 1032, F-67070 Strasbourg cedex, France

Received December 11, 2008

We report in this article one of the first examples of a reaction of O-demethylation carried out at a Fe(II) center by molecular dioxygen, in the homogeneous phase in non-porphyrinic chemistry. This reaction parallels at the intramolecular level a very important process found in biology leading to the derivatization and elimination of drugs by oxygen-dependent enzymes that contain nonheme iron centers. To get insight into some reactivity aspects of this reaction, we have used dioxygen and iron complexes coordinated to ligands that are substituted by methoxy groups. We detail in this work the coordination chemistry of FeCl₂ to the series of mono- (L₁), di- (L₂), and tris(2,3-dimethoxyphenyl) (L₃) α -substituted ligands in the tris(2-pyridylmethyl)amine series and the behavior of the complexes upon reaction with molecular dioxygen. As main outcomes of this study, we demonstrate that the methoxy group does not need to be coordinated to the metal center to undergo O-demethylation, but needs to be properly orientated close to an oxygenated form of the metal. We also demonstrate the importance of the environment in the reactivity with molecular dioxygen: whereas a regular 18-electron Fe(II) reacts with O₂, a five-coordinate, 16-electron center may be oxygen-stable, if the access of dioxygen to the reaction site is locked.

Introduction

The activation of dioxygen at inexpensive metal centers is of fundamental importance from both academic and applied points of view in the current economical context,^{1,2} for many groups expressing a renewed interest in the biomimetic approach.³ The presence of iron centers and dioxygen turns out to be crucial in many oxidation processes encountered in biology, in biosynthetic pathways, of course, but also in processes involving the metabolism of xenobiotics, further leading to their easy removal from living organisms after

modification of their structure.^{4–7} From this viewpoint, oxidative O-dealkylation is an important and well-known reaction in the metabolism of drugs, which is believed to occur at the metal site center during the catalytic cycle of heme-containing enzymes.^{8–10} In this context, nonheme proteins have by far been less-studied, although similar reactions were reported in early studies, sometimes as side- and undesired transformations,^{11,12} occasionally encouraging the setup of simple synthetic functional systems.^{13,14}

*To whom correspondence should be sent. Phone: 33-(0)390-241-537.

Fax: 33-(0)390-245-001. E-mail: mandon@chimie.u-strasbg.fr.

- (1) Labinger, J. A. *J. Mol. Catal. A* **2004**, *220*, 27–35.
- (2) Tong, J. H.; Li, Z.; Xia, C. G. *Prog. Chem.* **2005**, *17*, 96–110.
- (3) Special issue on dioxygen activation by metalloenzymes and models: *Acc. Chem. Res.*, 2007, *40*, 465–634.
- (4) Shikama, K. *Prog. Biophys. Mol. Biol.* **2006**, *91*, 83–162.
- (5) Kovacs, J. A. *Science* **2003**, *299*, 1024–1025.
- (6) Costas, M.; Mehn, M. P.; Jensen, M. P.; Que, L. Jr. *Chem. Rev.* **2004**, *104*, 939–986.
- (7) Neidig, M. L.; Solomon, E. D. *Chem. Commun.* **2005**, *47*, 6843–5863.

(8) Dowers, T. S.; Jones, J. P. *Drug Metab. Dispos.* **2006**, *34*, 1288–1290.

(9) Relling, M. V.; Nemeč, J.; Schuetz, E. G.; Schuetz, J. D.; Gonzalez, F. J.; Korzekwa, K. R. *Mol. Pharmacol.* **1994**, *45*, 352–358.

(10) Yu, A.; Dong, H.; Lang, D.; Haining, R. L. *Drug Metab. Dispos.* **2001**, *29*, 1362–1365.

(11) Funabiki, T.; Toyoda, T.; Ishida, H.; Tsujimoto, M.; Ozawa, S.; Yoshida, S. *J. Mol. Catal.* **1990**, *61*, 235–246.

(12) Mathieu, D.; Bartoli, J.-F.; Battioni, P.; Mansuy, D. *Tetrahedron* **2004**, *60*, 3855–3862.

(13) Katopodis, A. G.; Wilamasena, K.; Lee, J.; May, S. W. *J. Am. Chem. Soc.* **1984**, *106*, 7928–7935.

(14) Duprat, A. F.; Capdevielle, P.; Maumy, M. *J. Mol. Catal.* **1992**, *77*, L7–L11.

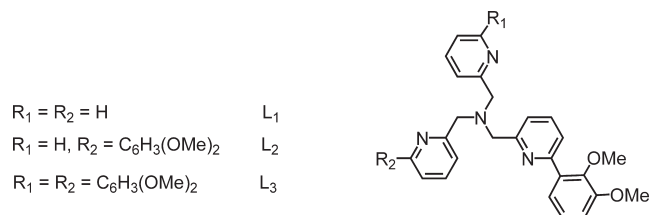


Figure 1. Ligands used in this study.

We are currently addressing the question of the iron–dioxygen interaction in ferrous complexes in which $FeCl_2$ is coordinated to α -substituted ligands in the tris(2-pyridylmethyl)amine (TPA) series.^{15–17} The general formation of μ -oxo diferric complexes is observed with two kinetically distinguishable steps upon reaction of dry molecular oxygen with the ferrous precursors.¹⁷ Acceleration of the reaction has been shown to occur upon increasing the electron deficiency at the metal center within a series of isostructural complexes with distorted octahedral geometries.¹⁷ Additionally and as expected, the presence of a vacant coordination site around the metal dramatically increases the reaction kinetics.^{16,17}

We already reported the preparation of the bis(2-[2,3-dimethoxy phenyl] 6-pyridylmethyl) (2-pyridylmethyl)amine ligand L_2 , drawn in Figure 1, as a precursor of the bis-catecholato α -substituted TPA for which the coordination chemistry was investigated.¹⁸ Using L_2 as a ligand in a class of oxygen-sensitive compounds, we expected that at least one methoxy group would lie close to the metal center, providing insight into the behavior of this noninnocent group under similar conditions, such as those present in biological systems. Additionally, methoxy-substituted phenyl groups can be considered as relatively bulky and electron-donating substituents,^{19,20} allowing comparison of the reactivity versus O_2 of the corresponding complexes with that of similar electron-deficient compounds.^{16,17} We thus started the preparation of the series of mono-, bis-, and tris-substituted ligands L_1 , L_2 , and L_3 and decided to test the reactivity of the corresponding $FeCl_2$ complexes versus dioxygen. The result is striking and is reported in this article. Whereas L_1FeCl_2 reacts slowly to yield a μ -oxo complex in a classical way, L_3FeCl_2 reacts only very poorly with dioxygen, in spite of a coordinatively trigonal bipyramidal unsaturated geometry. This very low sensitivity is due to a particular environment hampering coordination of O_2 to the metal center. The case of L_2FeCl_2 is unique since it reacts smoothly, yielding a dinuclear complex in which the ligand has undergone O-demethylation in the ortho position of the substituent. This compound is easily reduced, and the crystal structure of the diferric corresponding complex is reported. The present manuscript describes one of the very few examples of

O-demethylation carried out under homogeneous conditions upon reaction with O_2 with a ferrous nonporphyrinic complex. Additionally, we bring evidence that this reaction involves an initial coordination of dioxygen followed by a regioselective process, with no need for the methoxy group to coordinate to the metal center. This particular reaction can be considered as a salient extension of the nonheme chemistry of an important reaction already known in P450 chemistry.

Experimental Section

General Considerations. Chemicals were purchased from Aldrich Chemicals and used as received. Precursor ligands $BrTPA$, Br_2TPA , and Br_3TPA were prepared according to published procedures: Chuang, C. L.; Dos Santos, O.; Xu, X.; Canary, J. W. *Inorg. Chem.*, **1997**, *36*, 1967–1972. Ligand L_2 was prepared following the procedure described in ref 18. All solvents used during the metalation reactions and workup were distilled and dried according to the procedure given in W. L. F. Armarego, W. L. F.; Perrin, D. D. *Purification of Laboratory Chemicals*, 4th ed.; Pergamon Press: Oxford, U. K., 1997.

Analytical anhydrous $FeCl_2$ was obtained as a white powder by reacting iron powder (ACS grade) with hydrochloric acid in the presence of methanol under an argon atmosphere. Preparation and handling of all compounds (even L_3FeCl_2 , which is air stable) were performed under an argon atmosphere using Schlenk techniques, following standard procedures. The purity of the dry dioxygen was 99.99999% (grade 5). Zinc amalgam was prepared as already described in ref 17. Elemental analyses were carried out by the Service d'Analyses de la Fédération de Recherche de Chimie, Université Louis Pasteur, Strasbourg, France, and by the Service Central d'Analyses du CNRS, Solaize, France. Mass spectroscopy experiments were carried out by the Service Commun de Spectrométrie de Masse de l'Institut de Chimie de Strasbourg.

Physical Methods. 1H NMR data were recorded in CD_3CN for the complexes and $CDCl_3$ for the ligands at ambient temperature on a Bruker AC 300 spectrometer at 300.1300 MHz using the residual signal of CD_2HClN ($CHCl_3$) as a reference for calibration. The UV–vis spectra were recorded on a Varian Cary 05 E UV–vis NIR spectrophotometer equipped with an Oxford instrument DN1704 cryostat, using optically transparent Schlenk cells. Conductivity measurements were carried out under argon at 20 °C with a CDM 210 Radiometer Copenhagen Conductivity Meter, using a Tacussel CDC745-9 electrode. Cyclic voltammetry measurements were obtained from a PAR 173A potentiostat in a 0.1 M acetonitrile solution of $TBAPF_6$ (supporting electrolyte), using platinum electrodes and a saturated calomel electrode as a reference. For each measurement, the potential was checked by the addition of a small amount of ferrocene ($Fc/Fc^+ = 0.380$ v/SCE) in the cell.

Synthesis of L_1 : Mono(2-[2,3-dimethoxy Phenyl] 6-Pyridylmethyl) Bis(2-pyridylmethyl)amine. $BrTPA$ (794 mg, 2.15 mmol) and $Pd(PPh_3)_4$ (181 mg, 0.15 mmol) were suspended under argon in degassed toluene (100 mL). Sodium carbonate (10 mL of a 2 M aqueous solution) and commercially available 2,3-dimethoxyphenylboronic acid (704 mg, 3.87 mmol) dissolved in ethanol (5 mL) were added under argon. The reaction mixture was refluxed under argon for 48 h. The orange-colored solution was then evaporated to dryness. The remaining oil was dissolved in methylene chloride, and this organic phase was washed with aqueous sodium carbonate and distilled water and dried over magnesium sulfate. After filtration and concentration by rotary evaporation, the medium was deposited at the top of a column filled with silica and mounted with acetone. The column was washed with diethyl ether and the compound eluted with acetone. A brownish oil (662 mg, 72%) was obtained. Elem anal. calcd for $C_{26}H_{26}N_4O_2$, %: C, 73.24; H, 6.10. Found, %: C, 72.80; H, 6.01. 1H NMR, δ , ppm, $CDCl_3$: 3.65 (s, 3H), 3.90 (s, 3H), 3.93 (s, 4H),

(15) Mandon, D.; Machkour, A.; Goetz, S.; Welter, R. *Inorg. Chem.* **2002**, *41*, 5363–5372.

(16) Machkour, A.; Mandon, D.; Lachkar, M.; Welter, R. *Inorg. Chem.* **2004**, *43*, 1545–1550.

(17) Thallaj, N. K.; Rotthaus, O.; Benhamou, L.; Humbert, N.; Elhabiri, M.; Lachkar, M.; Welter, R.; Albrecht-Gary, A.-M.; Mandon, D. *Chem.—Eur. J.* **2008**, *14*, 6742–6753.

(18) Machkour, A.; Thallaj, N. K.; Benhamou, L.; Lachkar, M.; Mandon, D. *Chem.—Eur. J.* **2006**, *12*, 6660–6668.

(19) Jensen, M. P.; Lange, S. J.; Mehn, M. P.; Que, E. L.; Que, L. Jr. *J. Am. Chem. Soc.* **2003**, *125*, 2113–2128.

(20) He, Z.; Colbran, S. B.; Craig, D. *Chem.—Eur. J.* **2003**, *9*, 116–129. see also this reference for a good example of flexibility of a 2-5-dimethoxyphenyl substituted tripod in a copper complex.

3.95 (s, 2H), 6.93–6.94 (d, 1H), 6.96–6.97 (d, 1H), 7.11–7.14 (m, 2H), 7.15–7.17 (t, 1H), 7.34–7.35 (d, 1H), 7.36–7.37 (d, 1H), 7.52–7.55 (t, 1H), 7.62–7.66 (m, 2H), 7.69–7.70 (d, 2H), 8.52–8.53 (d, 1H), 8.54–8.55 (d, 1H). The trace is shown in the Supporting Information. MSES⁺: $m/z + \text{Li}^+ = 433.21$.

Synthesis of L₃: Tris(2-[2,3-dimethoxy Phenyl] 6-Pyridylmethyl) Amine. Br₃TPA (400 mg, 0.76 mmol) and Pd(PPh₃)₄ (41 mg, 0.035 mmol) were suspended under argon in degassed toluene (100 mL). Sodium carbonate (11 mL of a 2 M aqueous solution) and commercially available 2,3-dimethoxyphenylboronic acid (280 mg, 1.58 mmol) dissolved in ethanol (5 mL) were added under argon. The reaction mixture was refluxed under argon for several days, until no more Br₃TPA was detected by thin-layer chromatography (several days). The orange-colored solution was then evaporated to dryness. The remaining oil was dissolved in methylene chloride, and this organic phase was washed with aqueous sodium carbonate and distilled water and dried over magnesium sulfate. After filtration and concentration by rotary evaporation, the medium was deposited at the top of a column filled with silica and mounted with acetone. The column was washed with diethyl ether and the compound eluted with acetone. A brownish oil (320 mg, 61%) was obtained. Elem anal. calcd for C₄₂H₄₂N₄O₆, %: C, 72.19; H, 6.06. Found, %: C, 72.19; H, 5.98. ¹H NMR, δ , ppm, CDCl₃: 3.65 (s, 9H), 3.86 (s, 9H), 4.06 (s, 6H), 6.93–7.70 (m, 18H). The trace is shown in the Supporting Information. MSES⁺: $m/z + \text{H}^+ = 699.23$.

Preparation of the FeCl₂ Complexes. Details are given for L₁FeCl₂, but the following procedure applies to all complexes: 150 mg (0.35 mmol) of free L₁ was dissolved in a Schlenk tube containing 20 mL of dry and degassed THF. A total of 40 mg (0.31 mmol) of anhydrous FeCl₂ was dissolved in a second Schlenk tube containing 10 mL of dry and degassed THF. The solution of FeCl₂ was transferred under argon in the Schlenk containing the ligand, and the medium was stirred overnight. The solvent was then evaporated to dryness, and the compound was extracted with dry and degassed CH₃CN, filtered under an inert atmosphere, and concentrated. The addition of diethyl ether afforded a yellow solid, which was washed thoroughly with this solvent, prior to being dried under vacuum conditions. A total of 140 mg (82%) of L₁FeCl₂ with good analytical and spectroscopic data could be obtained. Spectroscopic data are detailed in the text and shown in the Supporting Information.

Oxygenation of L₂FeCl₂. A total of 150 mg (0.22 mmol) of the ferrous complex was dissolved under argon in 50 cm³ of CH₃CN in a Schlenk tube. Dry dioxygen was bubbled for 15 s, and the medium was kept under oxygen in the stopped Schlenk and stirred over 48 h. The solvent was evaporated. The dark-green solid was then thoroughly washed with diethyl ether and dried under vacuum conditions. At this stage, the diethyl ether fractions were collected and evaporated to dryness. The ¹H NMR spectrum of this colorless remaining material (ca. 50 mg) corresponded to pure L₂ ligand (superimposable spectroscopic NMR data). No trace of L₂* (modified ligand) could be detected by mass spectroscopy, the only signal being that of L₂ + H⁺ at $m/z = 563.29$. The dark-green material was recrystallized from CH₃CN/Et₂O to afford 70 mg of a microcrystalline dark-green solid, corresponding to a 78% yield based on the formula given below. Spectroscopic data are detailed in the text and shown in the Supporting Information.

Elem anal. calcd for C₃₃H₃₂N₄O₅Cl₄Fe₂, %: C, 48.45; H, 3.94; N, 6.85; Fe, 13.65; Cl, 17.33. Found, %: C, 48.09; H, 4.33; N, 6.66; Fe, 13.01; Cl, 16.81.

MSES⁺: $m/z = 638.1325$, C₃₃H₃₁ClFeN₄O₄⁺. Molecular conductivity value at $c = 5 \cdot 10^{-3} \text{ mol L}^{-1}$: $\Lambda = 86 \text{ S mol}^{-1} \text{ cm}^2$.

The addition of dilute Et₃N to a solution of this compound in CH₃CN resulted in the loss of the ligand-to-metal charge transfer (LMCT) absorption and a continuous absorption increase between 580 and 320 nm, in line with the occurrence of a deprotonation process. This observation, together with the absence of any

free OH⁻ signal in IR spectroscopy, strongly supports the presence of the [L₂*Fe–OH–FeCl₃]⁺Cl⁻ structure. All spectroscopic data are shown in the Supporting Information.

Preparation of L₂*FeCl₃. A total of 100 mg (0.12 mmol) of the green compound was dissolved under argon in CH₃CN. The solution was transferred into a Schlenk tube containing several drops of 10% zinc amalgam. The medium was stirred and became bright orange over 10 min. This solution turned out to be extremely oxygen-sensitive, becoming dark violet in the case of a leak into the reaction vessel. The addition of diethyl ether allowed precipitation of an orange solid material, which was recrystallized from CH₃CN/Et₂O. A total of 80 mg was obtained, corresponding to an 83% yield. Even in the solid state, this compound is difficult to handle. We believe that this is the reason why a satisfactory elemental analysis could not be obtained. Elem anal. calcd for C₃₃H₃₁Cl₃Fe₂N₄O₄, %: C, 51.73; H, 4.05; Fe, 14.63; Cl, 13.91. Found, %: C, 50.21; H, 3.82; Fe, 13.17; Cl, 13.05. Spectroscopic data are detailed in the text and shown in the Supporting Information.

Single crystals were obtained by slow diffusion of diethyl ether in a sealed tube containing a CH₃CN solution of L₂FeCl₂, a CH₃CN solution of L₂*Fe₂Cl₃, and a THF solution of L₃FeCl₂. Single crystals of [L₁FeCl₂]₀ were obtained by layering with diethyl ether a CH₃CN solution of L₁FeCl₂ that was previously oxygenated.

X-Ray Analysis. Single crystals of [L₁FeCl₂]₂O·CH₃CN, L₂FeCl₂, L₃FeCl₂·THF, and L₂*Fe₂Cl₃·OEt₂ were mounted on a Nonius Kappa-CCD area detector diffractometer (Mo K α , $\lambda = 0.71073 \text{ \AA}$). Quantitative data were obtained at 173 K for all complexes. The complete conditions of data collection (Denzo software) and structure refinements are given in the Supporting Information. The cell parameters were determined from reflections taken from one set of 10 frames (1.0° steps in ϕ angle), each at 20 s exposure. The structures were solved using direct methods (SIR97) and refined against F^2 using the SHELXL97 software (*Kappa CCD Operation Manual*; Nonius B.V.: Delft, The Netherlands, 1997. Sheldrick, G. M. *SHELXL97*; University of Göttingen: Göttingen, Germany, 1997). The absorption was not corrected. All non-hydrogen atoms were refined anisotropically. Hydrogen atoms were generated according to stereochemistry and refined using a riding model in SHELXL97.

Crystal Data for [L₁FeCl₂]₂O·CH₃CN. Red crystals, monoclinic, space group $C 2/c$, $a = 34.5912(13) \text{ \AA}$, $b = 12.9475(6) \text{ \AA}$, $c = 12.7992(4) \text{ \AA}$, $\beta = 103.575(2)^\circ$, $V = 5572.2(4) \text{ \AA}^3$, $D_{\text{calcd}} = 1.436 \text{ g cm}^{-3}$, $Z = 4$. For 8083 unique observed reflections with $I > 2\sigma(I)$ and 351 parameters, the discrepancy indices are $R = 0.0915$ and $R_w = 0.2469$.

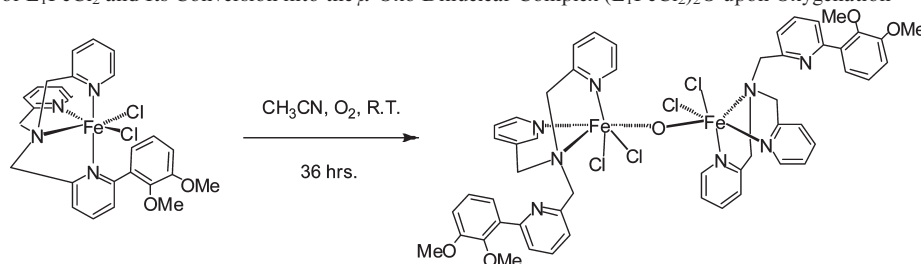
Crystal Data for L₂FeCl₂. Yellow crystals, monoclinic, space group $P2_1/c$, $a = 9.004(5) \text{ \AA}$, $b = 28.319(5) \text{ \AA}$, $c = 12.962(5) \text{ \AA}$, $\beta = 104.882(5)^\circ$, $V = 3194(2) \text{ \AA}^3$, $D_{\text{calcd}} = 1.434 \text{ g cm}^{-3}$, $Z = 4$. For 9282 unique observed reflections with $I > 2\sigma(I)$ and 406 parameters, the discrepancy indices are $R = 0.0445$ and $R_w = 0.0897$.

Crystal Data for L₃FeCl₂·THF. Yellow crystals, orthorhombic, space group $Pbca$, $a = 15.7653(3) \text{ \AA}$, $b = 22.9257(3) \text{ \AA}$, $c = 2426.43(4) \text{ \AA}$, $V = 8769.9(2) \text{ \AA}^3$, $D_{\text{calcd}} = 1.305 \text{ g cm}^{-3}$, $Z = 4$. For 11669 unique observed reflections with $I > 2\sigma(I)$ and 523 parameters, the discrepancy indices are $R = 0.0584$ and $R_w = 0.1778$.

Crystal Data for L₂*Fe₂Cl₃·OEt₂. Yellow crystals, orthorhombic, space group $P2_12_12_1$, $a = 12.397(3) \text{ \AA}$, $b = 14.716(3) \text{ \AA}$, $c = 20.345(5) \text{ \AA}$, $V = 3711.6(15) \text{ \AA}^3$, $D_{\text{calcd}} = 1.437 \text{ g cm}^{-3}$, $Z = 4$. For 8399 unique observed reflections with $I > 2\sigma(I)$ and 431 parameters, the discrepancy indices are $R = 0.0608$ and $R_w = 0.1477$.

Results

Ligands L_{1–3} (see Figure 1) were prepared by the reaction of 2,3-dimethoxyphenylboronic acid with the

Scheme 1. Structure of L_1FeCl_2 and Its Conversion into the μ -Oxo Dinuclear Complex $(L_1FeCl_2)_2O$ upon Oxygenation

α -bromo-substituted tripods, following the procedure already published for L_2 .¹⁸ The cyclic voltammetry curves of all ligands display an irreversible anodic wave at a potential that remains invariant at $E_a \approx 1.05$ V/SCE. Another anodic wave is observed at $E_a \approx 1.50$ V/SCE with variable intensity patterns along the L_{1-3} series, assigned to the oxidation of the methoxy groups.

Structure of the Complexes. The preparation of the complexes follows the classical procedure, involving the reaction of 1 equiv of $FeCl_2$ with a slight excess of the ligand.¹⁵ The stable complexes thus obtained are characterized by elemental analyses and in solution by UV–visible spectroscopy, 1H NMR, cyclic voltammetry, and molecular conductivity. The molecular structure of L_1FeCl_2 is deduced from spectroscopic data and electrochemical measurements, including conductimetry. In the solid state, X-ray diffraction structures have been obtained for L_2FeCl_2 and L_3FeCl_2 .

L_1FeCl_2 . The presence of a distinguishable MLCT absorption at $\lambda = 376$ nm ($\epsilon = 1.0 \cdot 10^3$ mmol⁻¹ cm²) together with a typical 1H NMR paramagnetic spectrum supports tetradentate coordination of the tripod in this complex.^{15,21,22} At a concentration of 4 mM, the molecular conductivity value is $\Lambda = 46$ Scm² mol⁻¹, indicating a neutral electrolytic behavior. In cyclic voltammetry, a single wave is observed at $E_{1/2} = 184$ mV/SCE, with a pseudoreversible pattern, $\Delta E = 84$ mV and $I_{pc}/I_{pa} = 0.80$, in line with the presence of a distorted O_h geometry. The 1H NMR spectrum displays typical patterns (chemical shifts and mid-intensity width) of distorted O_h high-spin $FeCl_2$ complexes with monosubstituted tripods. The trace is given in the Supporting Information. We thus believe that the metal center lies in a distorted octahedral geometry, in solution and in the solid state as well, as drawn in Scheme 1.

L_2FeCl_2 . The 1H NMR spectrum is very similar to that of the complex with the parent [bis(2-phenyl 6-pyridylmethyl) (2-pyridylmethyl)]amine.¹⁵ The main difference lies in the presence of signals from the methoxy groups at $\delta = 15$ ppm. The weak MLCT absorption at $\lambda = 368$ nm ($\epsilon = 0.75 \cdot 10^3$ mmol⁻¹ cm²) together with the 4 mM molecular conductivity value of $\Lambda = 47$ Scm² mol⁻¹ indicate a five-coordinate geometry in this complex. All spectroscopic data are given in the Supporting Information. The cyclic voltammogram of this complex consists of one reversible wave at $E_{1/2} = 8$ mV/SCE standing for L_2FeCl_2 , with $\Delta E = 80$ mV and $I_{pc}/I_{pa} = 0.95$, together

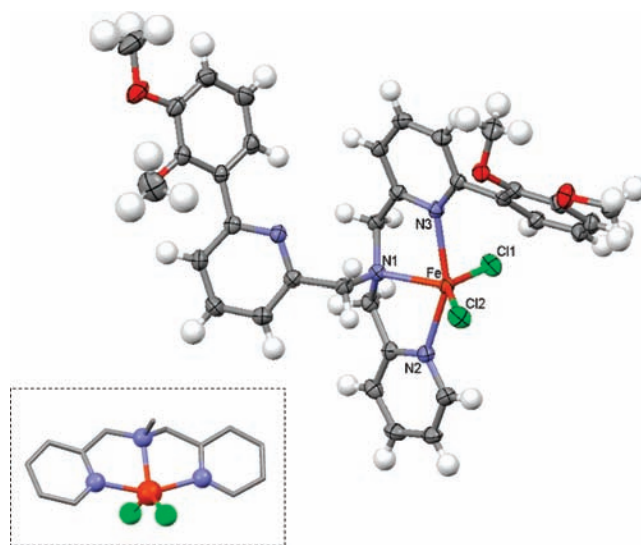


Figure 2. Mercury drawing of complex L_2FeCl_2 . Principal distances (in Å) and angles (in deg): FeN1, 2.1675(19); FeN2, 2.224(2); FeN3, 2.266(2); FeCl1, 2.3248(10); FeCl2, 2.2656(10); N2FeN3, 154.65(7); N1FeCl1, 100.11(5); N1FeCl2, 122.09(5); Cl2FeCl1, 137.56(3).

with another pseudo-reversible wave at $E_{1/2} = 340$ mV/SCE, assigned to the presence of the dissociated monocation $[L_2FeCl(MeCN)]^+$, Cl^- in equilibrium under the conditions of the measurement.²¹

The X-ray crystal structure of L_2FeCl_2 could be solved, and a Mercury drawing is displayed in Figure 2. In L_2FeCl_2 , the tripod acts as a tridentate ligand, one of the substituted pyridines being remote from the coordination center.

A five-coordinate metal center generally exhibits square-pyramidal or trigonal-bipyramidal geometries.²³ In L_2FeCl_2 , the calculated trigonality index is $\tau = 0.28$. In this structure, all metal-to-ligand distances lie above 2.0 Å, in line with a high-spin state for the metal center.

L_3FeCl_2 . The 1H NMR spectrum is not informative, with a prominent signal emerging at $\delta \approx 0.5$ ppm over a broad envelope lying between +10 and -5 ppm. The absence of any well-defined MLCT absorption in the UV–visible region is reminiscent of the spectra observed in complexes with ligands in which all three α positions are substituted.^{16,21} The 4 mM molecular conductivity value of $\Lambda = 23$ Scm² mol⁻¹ indicates a neutral electrolytic behavior of the complex. The cyclic voltammogram of this complex consists of only one reversible wave at $E_{1/2} = 9$ mV/SCE with $\Delta E = 100$ mV and $I_{pc}/I_{pa} = 0.90$.

(21) Benhamou, L.; Lachkar, M.; Mandon, D.; Welter, R. *Dalton Trans.* **2008**, 6996–7003.

(22) Machkour, A.; Mandon, D.; Lachkar, M.; Welter, R. *Inorg. Chim. Acta* **2005**, 358, 839–843.

(23) Addison, A. W.; Nageswara, R.; Reedijk, J.; Van Rijn, J.; Verschoor, G. C. *J. Chem. Soc., Dalton Trans.* **1984**, 1349–1355.

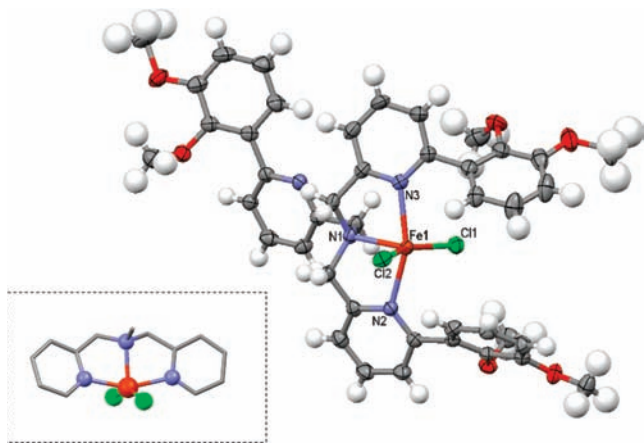


Figure 3. Mercury view of complex L_3FeCl_2 . Principal distances (in Å) and angles (in deg): FeN1, 2.183(2); FeN2, 2.235(2); FeN3, 2.205(2); FeCl1, 2.2930(8); FeCl2, 2.3576(7); N2FeN3, 156.89(8); N1FeCl1, 108.62(6); N1FeCl2, 98.66(6); Cl2FeCl1, 152.61(3).

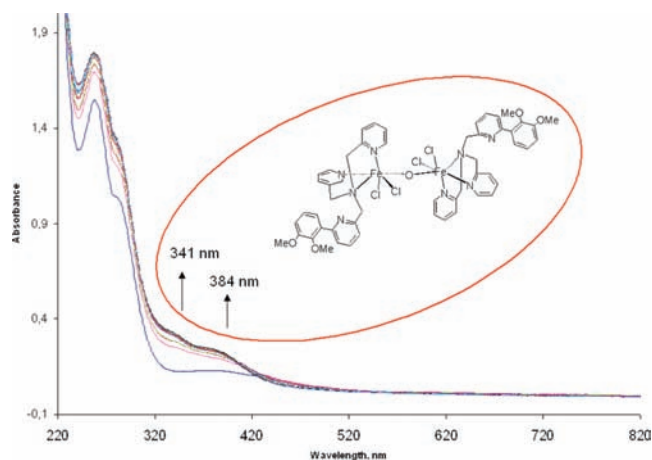


Figure 4. Spectral absorption changes versus time in the course of oxygenation of complex L_1FeCl_2 over the first 16 h (1 scan/h). From the 16th hour, the reaction goes on, but precipitation occurs in the cuvette, yielding poorly tractable data, not shown on this graph.

Single crystals could be obtained for L_3FeCl_2 , and the Mercury diagram is displayed in Figure 3.

Here again, the tripod coordinates in the tridentate mode with one dangling substituent. The distortion versus ideal trigonal-bipyramidal is important, with $\tau = 0.07$, although the observed geometry is not planar, as seen from Figure 3 (inset). This point will be discussed later. In this complex also, all metal-to-ligand distances lie above 2.0 Å, in line with a high-spin state for the metal center.

Reactivity with O_2 . L_1FeCl_2 . When exposed to dry dioxygen, the color of this compound gradually turned to brownish green. Monitoring the oxygenation by UV–vis allowed for the detection of signals at $\lambda = 341$ and 384 nm, typical of μ -oxo diferric complexes. The reaction goes slowly, and a poorly soluble compound is obtained. At a preparative scale, the reaction is complete over 40–48 h after the addition of dioxygen. Figure 4 shows the spectral absorption changes versus time in the course of oxygenation of complex L_1FeCl_2 .

Single crystals of $(L_1FeCl_2)_2O$ could be obtained. As expected from the UV–vis measurements, the compound displays the μ -oxo diferric structure. The ligand

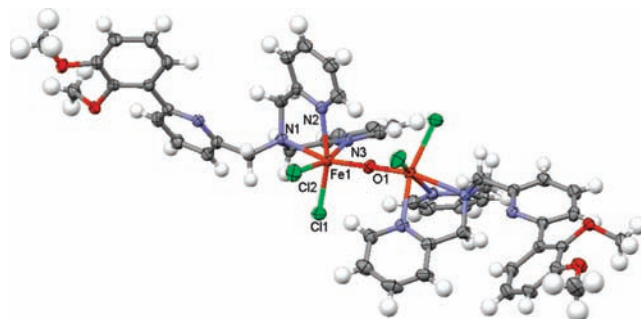


Figure 5. Mercury view of complex $(L_1FeCl_2)_2O$. Principal distances (in Å) and angles (in deg): FeN1, 2.387(4); FeN2, 2.172(5); FeN3, 2.208(5); FeCl1, 2.3361(17); FeCl2, 2.3580(17); FeO1, 1.7885(7); FeO1Fe1, 175.9(4). Distance Fe1–Fe1: 3.575(7). Torsion angles Cl1Fe1Fe1Cl2 = Cl2Fe1Fe1Cl1: 124.7°.

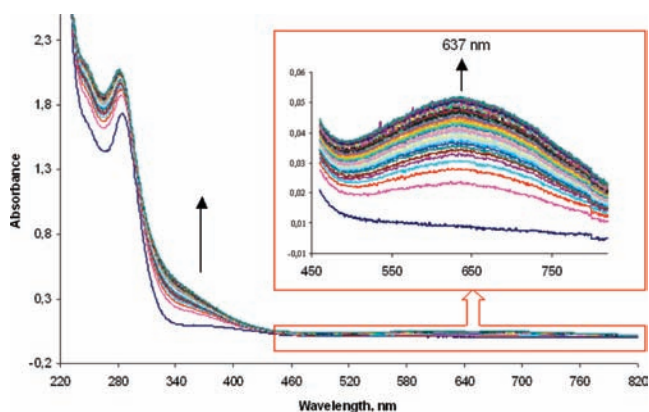


Figure 6. Spectral absorption changes versus time in the course of oxygenation of complex L_2FeCl_2 . One scan every 60 min over 36 h. Inset: the 450–820 nm range, showing the appearance of the LMCT absorption at $\lambda = 637$ nm.

coordinates in the tridentate mode, the substituted pyridine being remote from the metal center. The geometry around the metal is pseudo-octahedral, with two chloride atoms and one oxo bridge completing the coordination sphere. As a consequence, $(L_1FeCl_2)_2O$ is a neutral molecule. A mercury diagram is displayed in Figure 5.

The structural parameters are close to those already reported for the isostructural $(FTPAFeCl_2)_2O$,¹⁷ with d (Fe1–Fe2) = 3.57 Å and \angle Fe1OFe2 = 175.9°.

L_3FeCl_2 . Solutions of this complex in acetonitrile or in THF could be handled under atmospheric conditions for several hours without alteration. Bubbling dry dioxygen in the solution resulted in the progressive appearance of brownish green shades that became distinguishable only over one day of stirring. Monitoring the absorbance by UV–visible spectroscopy over 60 h allowed for the detection of a 10–15% increase in absorbance around 350 nm. No spectroscopic modification was observed in the 400–820 nm range. The data are shown in the Supporting Information.

L_2FeCl_2 . Upon exposure to dry dioxygen, the yellow solution of the complex turned deep green. UV–visible spectroscopy allowed progressive detection of a broad absorption at $\lambda = 637$ nm ($\epsilon = 0.41 \cdot 10^3 \text{ mmol}^{-1} \text{ cm}^2$, based on the initial concentration of L_2FeCl_2), similar to the LMCT $ArO \rightarrow Fe^{(III)}$ band observed in a catecholato complex,¹⁸ as shown in Figure 6. Noteworthy is the fact that no tractable absorption could be detected within the

300–400 nm range. In contrast with L_3FeCl_2 , the change in color became obvious over 1 to 2 h. The reaction was considered as complete over 30–36 h.

Monitoring the oxygenation reaction by 1H NMR resulted in a progressive loss of the signal of the Fe(II) complex, no new tractable species being detected in the paramagnetic region. Release of the free ligand, however, was observed in the diamagnetic area. In order to make sure that these spectroscopic modifications were not the result of any partial degradation process, we ran this reaction on the preparative scale. After workup, a dark green microcrystalline solid could be isolated, with a 78% yield based on the $C_{33}H_{32}Cl_4Fe_2N_4O_5$ formulation (vide infra). On the other hand, almost 50% (based on the amount of starting complex) of free and unmodified ligand L_2 was recovered in the washing phases. Mass spectroscopy analysis of the green compound allowed detection of the $[L_2^*FeCl]^+$ cation at $m/z = 638.15$ as the main signal, with L_2^* being a modified ligand in which one methyl group has been lost. However, the description of this green complex as a ferric mononuclear compound does not correspond to the results of the elemental analysis. The molar element ratios indicate the presence of a dinuclear asymmetric complex ($L_2^*/Fe/Cl = 1:2:4$). The found elemental percentages (%), C = 48.09, H = 4.33, N = 6.66, Fe = 13.01, and Cl = 16.8, match those obtained from the $C_{33}H_{32}Cl_4Fe_2N_4O_5$ formulation with the calculated values (%) C = 48.45, H = 3.94, N = 6.85, Fe = 13.65, and Cl = 17.33. The molecular conductivity indicates that the compound behaves as a monocharged species with $\Lambda = 86 \text{ S mol}^{-1} \text{ cm}^2$ at a concentration of $5 \times 10^{-3} \text{ mol L}^{-1}$. Thus, two structural hypotheses can be drawn, $[L_2^*Fe-Cl-FeCl_3]OH$ (A) or $[L_2^*Fe-OH-FeCl_3]Cl$ (B). The IR spectrum of the green compound (shown in the Supporting Information) points out the lack of vibration assigned to “free” OH^- . By contrast, a very weak signal is observed at 3650 cm^{-1} which might fit with the presence of a bridging OH group. Furthermore, our green compound is sensitive to basic media, reacting with Et_3N . Considered together, these observations support structure B, $[L_2^*Fe-OH-FeCl_3]Cl$, as the most likely hypothesis.

Cyclic voltammetry experiments on the green compound afforded two reduction waves: a reversible one was observed at $E_{1/2} = -80 \text{ mV/SCE}$ with $\Delta E = 80 \text{ mV}$ and $I_{pc}/I_{pa} = 1.0$; the second irreversible wave was detected at $E_c = -500 \text{ mV/SCE}$.

Full reduction of the green complex with zinc amalgam under anaerobic conditions in a THF or CH_3CN solution afforded, over 10 min, a bright orange solution, which turned out to be extremely oxygen-sensitive.

This reaction was carried out on a preparative scale, and a bright orange solid could be isolated after treatment with an 83% yield. The 1H NMR spectrum of this complex displays paramagnetically shifted signals within the -40 to $+150 \text{ ppm}$ range (the spectrum is displayed in the Supporting Information). We later could obtain single crystals of this compound and checked that the data obtained from the bulk synthesis were identical to those recorded from hand-picked single crystals. Thus, this reduction reaction turned out to be clean. The striking point is the extreme oxygen sensitivity of this compound which, even in the solid state, becomes dark within a few seconds.

The UV–visible spectrum of this new species, shown in Figure 7, displayed no characteristic feature in the 500–800 nm region. A new absorption at $\lambda = 377 \text{ nm}$ ($\epsilon = 1.39 \times 10^3 \text{ mmol}^{-1} \text{ cm}^2$) is present, reminiscent of that observed in the catecholato complex already mentioned above.¹⁸

The color, spectroscopic features, and extreme sensitivity to dioxygen strongly suggested coordination of a phenolate derivative to Fe(II).

This was confirmed by the molecular structure of this yellow–orange compound, as single crystals of the compound termed $L_2^*Fe_2Cl_3$ could be obtained. A Mercury diagram is displayed in Figure 8.

This new complex is a dinuclear di-Fe(II) compound, with an asymmetric structure: only one ligand is present for two iron atoms. As expected, the L_2 ligand in the original ferrous complex has undergone O-demethylation, becoming L_2^* . In $L_2^*Fe_2Cl_3$, one iron atom lies in a pseudo-octahedral geometry, being coordinated by the four nitrogen atoms from the ligand, one bridging

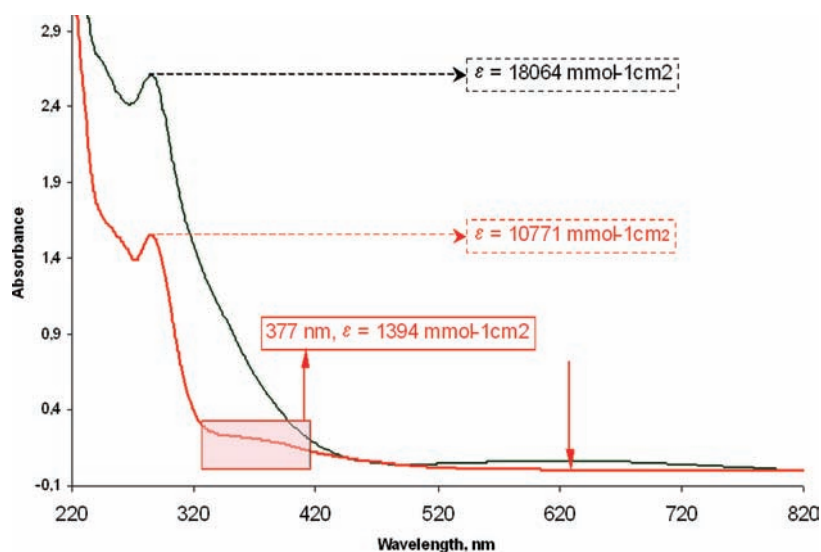


Figure 7. Spectral absorption changes upon Zn/Hg reduction of a $1.4 \times 10^{-3} \text{ M}$ solution of the green compound over 10 min.

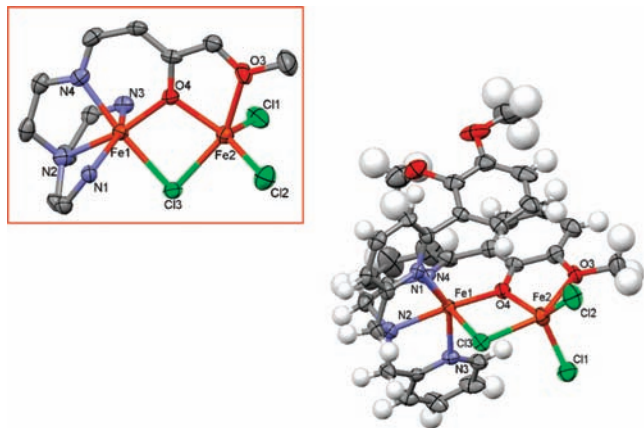


Figure 8. Mercury view of complex $L_2^*Fe_2Cl_3$. Principal distances (in Å) and angles (in deg): Fe1N1, 2.238(5); Fe1N2, 2.189(5); Fe1N3, 2.265(5); Fe1N4, 2.139(5); Fe1Cl3, 2.4546(17); Fe1O4, 1.983(4); Fe2Cl3, 2.4778(17); Fe2O4, 2.074(4); Fe2O3, 2.230(4); Fe2Cl2, 2.313(2); Fe2Cl1, 2.296(2); N4Fe1Cl3, 174.45(14); O4Fe1Cl3, 85.97(11); Fe1Cl3Fe2, 83.09(5); Cl3Fe2O4, 83.47(11); Fe2O4Fe1, 107.45(17). Distance Fe1–Fe2: 3.274(7).

chloride atom, and a bridging phenolato oxygen atom that originates from the bis(methoxy)phenyl arm of the ligand. All Fe–N distances lie above 2.1 Å; the phenolato is tightly bound with $d(Fe1-O4) = 1.983$ Å. The bridging chloride lies at $d(Fe1-Cl3) = 2.455$ Å. The second iron atom is coordinated by the bridging chloride with $d(Fe2-Cl3) = 2.478$ Å, the bridging phenolato oxygen atom with $d(Fe2-O4) = 2.074$ Å, one oxygen atom from a methoxy group with $d(Fe2-O3) = 2.229$ Å, and two terminal chloride ligands with $d(Fe2-Cl2) = 2.313$ Å and $d(Fe2-Cl1) = 2.296$ Å. This five-coordinated environment provides the metal center with a severely distorted square-pyramidal environment, with $\tau = 0.31$. The metal-to-metal distance is 3.271 Å.

Discussion

Structures of the Complexes. L_1FeCl_2 . The spectroscopic features that characterize distorted octahedral geometry for similar complexes in solution are now well-known. For this complex, all spectroscopic data support the occurrence of such a geometry: pronounced MLCT absorption, 1H NMR data with sharp paramagnetic signals, and neutral electrolytic behavior in solution.^{15,17,21,22} Obviously, in the present case, as in other similar complexes,¹⁹ the steric hindrance provided by a single aromatic substitution remains weak, not being strong enough to induce decoordination of the substituted pyridine. Thus, the metal center lies in the classical geometry usually encountered for Fe(II) complexes. Moreover, the $E_{1/2} = 184$ mV value found in electrochemistry lies, as expected, slightly below that measured from the distorted O_h parent $TPAFeCl_2$ complex.²¹

Solution Studies of L_2FeCl_2 and L_3FeCl_2 . All spectroscopic data support the presence of a five-coordinate species in solution.^{15,16,21} The 1H NMR spectrum of L_2FeCl_2 is very similar to that obtained from $[(C_6H_5)_2TPA]FeCl_2$ that exhibits a trigonal bipyramidal geometry in the solid state and in solution.¹⁵ We recently observed that the $FeCl_2$ complex with the Me_3TPA ligand is cleanly converted into the bis-acetonitrile dication when dissolved in a strongly dissociative medium, such

as those used for electrochemical measurements.²¹ The presence of two waves with L_2FeCl_2 is probably due to an equilibrium between the L_2FeCl_2 form (low positive potential, $E_{1/2} = 8$ mV/SCE) and the dissociated mono-anion $[L_2FeCl(MeCN)]^+$, Cl^- form (high positive potential, $E_{1/2} = 340$ mV/SCE). The single wave observed for L_3FeCl_2 at a low positive potential ($E_{1/2} = 9$ mV/SCE) strongly suggests that only one species is present and that the structure observed in the solid state is completely retained in the electrochemical solution. In these complexes, the reason for a possible equilibrium (L_2FeCl_2) or not (L_3FeCl_2) might be related to the effect of aromatic substituents close to the metal (vide infra). Anyway, the low positive potential values are consistent with a higher electron density at the metal center, in line with hypodentate coordination of the ligand. Thus, even indirectly, electrochemical measurements can be useful tools for geometry predictions.²¹

Structures of L_2FeCl_2 and L_3FeCl_2 . Hypodentate²⁴ coordination of various tripods within the TPA family^{25,26} to iron is now well-known, leading to complexes in which the metal lies in a trigonal-bipyramidal environment,^{15,16,27,28} or square-pyramidal in a particular case.³⁰ Tridentate coordination of the ligand is found in L_2FeCl_2 and L_3FeCl_2 . The values of the τ index suggest square-pyramidal geometries rather than trigonal-bipyramidal. However, the trans-pyridyl angles (axial direction for determination of τ) open in the wrong direction, with relatively invariant values typically in the 152–157° range within the series of isostructural characterized complexes.^{15,16,21} This obviously moderates the significance of the τ parameter in our case. The value of the $\langle Cl_1FeCl_2$ angle seems to be more indicative of distortions.

L_2FeCl_2 . In this complex, $\langle Cl_1FeCl_2 = 137.6^\circ$, that is, the average of the values found within the series of isostructural complexes.^{15,16,21,22} It is noteworthy that a repulsion occurs between the Cl2 chloride and the *o*-OMe group of the substituent, as can be seen in Figure 9 (left). As a consequence, the structure is open, providing full lateral access to the metal center.

L_3FeCl_2 . In this complex, the value of $\langle Cl_1FeCl_2 = 152.6^\circ$ corresponds to the most open angle found for such complexes. A careful examination of the structure provides rationale for this: both chloride ligands lie in a position where they interact with hydrogen atoms from the methoxy groups and methylene, as shown in Figure 9 (right).

Correlatively, the two mean planes of the adjacent bis(methoxy)phenyl substituents are not coplanar, since the corresponding angle value is 62.3°. These aromatic arms define a narrow interstice leading to the metal, the shortest distance between these two aromatic substituents being $d(C25-C11) = 4.26$ Å. Under these conditions, and with a 5.59 Å intercentroid distance, only a weak

(24) Blackman, A. G. *C. R. Chim.* **2004**, *8*, 107–119.

(25) Blackman, A. G. *Polyhedron* **2005**, *24*, 1–39.

(26) Blackman, A. G. *Eur. J. Inorg. Chem.* **2008**, 2633–2647.

(27) Diebold, A.; Hagen, K. S. *Inorg. Chem.* **1998**, *37*, 215–223.

(28) Jo, D.-H.; Chiou, Y.-M.; Que, L.Jr. *Inorg. Chem.* **2001**, *40*, 3181–3190.

(29) Schueneman, V.; Jung, C.; Trautwein, A. X.; Weiss, R.; Mandon, D. *FEBS Lett.* **2000**, *479*, 149–154.

(30) Thallaj, N. K.; Machkour, A.; Mandon, D.; Welter, R. *New J. Chem.* **2005**, *29*, 1555–1558.

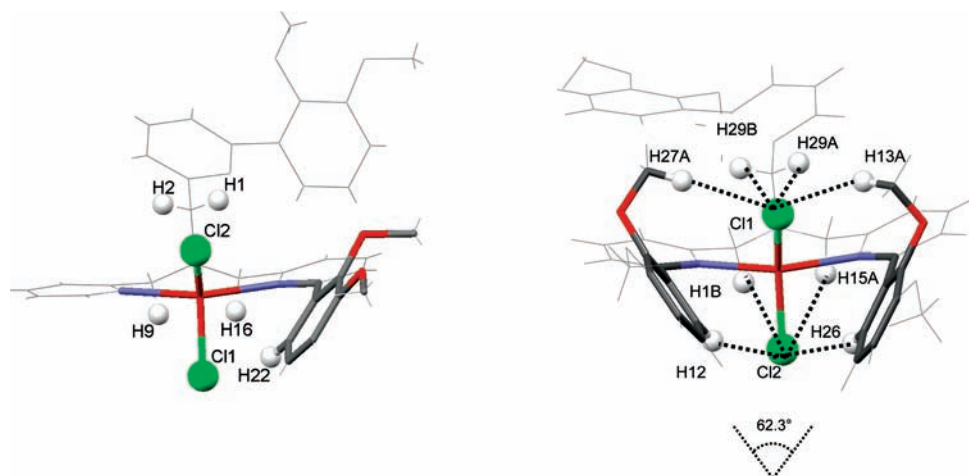


Figure 9. (Left) Structure of L_2FeCl_2 ; lateral view along the Cl_1FeCl_2 plane, showing access to the metal center. This structure is much more open than that of L_3FeCl_2 , providing easy access to the metal center. $d_{Cl_2-H_2} = 3.50$ Å; $d_{Cl_2-H_1} = 3.49$ Å; $d_{Cl_1-H_{22}} = 2.65$ Å; $d_{Cl_1-H_9} = 3.21$ Å; $d_{Cl_1-H_{16}} = 3.11$ Å. (Right) Structure of L_3FeCl_2 ; lateral view along the Cl_1FeCl_2 plane, showing access to the metal center. Short contacts between the chloride ligands and neighboring H atoms in L_3FeCl_2 : $d_{Cl_1-H_{29B}} = 3.33$ Å; $d_{Cl_1-H_{29A}} = 3.13$ Å; $d_{Cl_1-H_{27A}} = 2.76$ Å; $d_{Cl_1-H_{13A}} = 2.93$ Å; $d_{Cl_2-H_{11B}} = 3.07$ Å; $d_{Cl_2-H_{15A}} = 2.93$ Å; $d_{Cl_2-H_{12}} = 2.65$ Å; $d_{Cl_2-H_{26}} = 2.95$ Å.

potential π -stacking effect can be suspected.³¹ As drawn in Figure 9 (right), the global picture is that of a tweezer with two converging arms kept in position by hydrogen bonds, with the net effect of opening the $\angle Cl_1FeCl_2$ angle, while limiting the access to the metal center. This is in striking contrast with the situation in L_2FeCl_2 .

Reactivity versus Dioxygen: General Considerations. L_1FeCl_2 . $FeCl_2$ complexes react with dioxygen much better, as the metal center exhibits Lewis acidity character, that is, the ligands are electrodeficient.¹⁷ The bis(methoxy)phenyl substituted ligands presented in this study display anodic potential that is relatively invariant, typically $E_a \approx 1.05$ mV/SCE, slightly below the reported value of $E_a = 1.12$ mV/SCE found for the parent TPA ligand.¹⁷ The $E_{1/2} = 186$ mV value found for L_1FeCl_2 neighbors the $E_{1/2} = 195$ mV found in the parent $TPAFeCl_2$ complex. Therefore, the observed smooth oxygenation process is not surprising, although careful UV–visible monitoring is not possible because the end product is poorly soluble. We estimate however that the reaction is complete over 40–48 h, a reaction time slightly longer than that previously reported for the parent $TPAFeCl_2$ complex. The μ -oxo diferric complex obtained displays a structure similar to that obtained upon oxygenation of the complex with a monofluoro-substituted ligand in which the substituted arm of the tripod is uncoordinated.¹⁷

L_2FeCl_2 . This complex reacts smoothly with O_2 , the conversion rate reaching 90% over 30 h. This is considerably slower than what is observed with the isostructural $F_3TPAFeCl_2$ complex for which immediate conversion was reported.¹⁶ This might reflect the differences in the electronic properties of the corresponding ligands, since $E_a = 1.28$ mV/SCE for F_3TPA , that is, ≈ 250 mV higher than L_2 . Thus, L_2FeCl_2 , being more electron-rich than the isostructural complex with a fluorinated ligand, reacts slower than the latter.

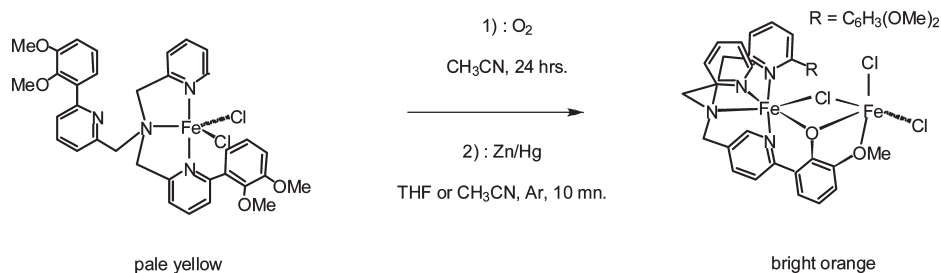
L_3FeCl_2 . The surprise came from the very low sensitivity of this complex, for which a reactivity similar to that of L_2FeCl_2 was expected. We already postulated that the

oxygenation reaction takes place via coordination of O_2 to the metal center.¹⁷ The fact that a five-coordinate environment accelerates the reaction is well-known and was experimentally demonstrated.^{16,17} We thus have here an exception. However, comparison of the two five-coordinate structures provides the clue to the unexpected lack of sensitivity of L_3FeCl_2 . From Figure 9 (left), it seems obvious that the access of exogenous ligands to the metal center is open in L_2FeCl_2 . The reaction goes slowly, but it works. Figure 9 (right) displays the lateral view, showing the access to the iron center in L_3FeCl_2 . As already stated above, the particular orientation of the two bis(methoxy)phenyl groups is not due to chance but results from stabilization because of methoxy/chloride interaction. The result is that the converging aromatic arms delineate a sterically hindered nonpolar environment. As a consequence, access to the iron center is dramatically restricted, even for a small molecule such as O_2 . In biological systems, controlling access of small molecules to active sites by the proteic environment is an obvious fact. In large synthetic systems, an elegant demonstration has recently been reported: a reduction in activity versus O_2 of synthetic non-heme iron sites is observed when those are buried in dendrimers.³² Far below in size and structure, the case of L_3FeCl_2 illustrates such a principle. We postulate that the poor reactivity of this complex is simply due to overprotected access to the metal center by its particular aromatic environment.

O-Demethylation in L_2FeCl_2 . μ -Oxo diferric compounds generally display a brownish color. Thus, the appearance of a dark green color upon oxygenation of L_2FeCl_2 was surprising and strongly suggested the presence of a coordinated phenolate at the ferric site. We obviously checked that what was detected in spectroscopy corresponded indeed to a major reaction easily being carried out on the preparative scale. In order to elucidate the structure of the dark green reaction product, we tried for a long time to grow single crystals, without success.

(31) Spek, A. L. *J. Appl. Cryst.* **2003**, *36*, 7–13.

(32) Zhao, M.; Helms, B.; Slonkina, E.; Friedle, S.; Lee, D.; DuBois, J.; Hedman, B.; Hodgson, K. O.; Fréchet, J. M. J.; Lippard, S. *J. Am. Chem. Soc.* **2008**, *130*, 4352–4363.

Scheme 2. The Two-Step Conversion of L_2FeCl_2 into $L_2^*FeCl_3$ ^a

^a The total yield of the reaction is 64% relative to the starting Fe(II) complex.

The ¹H NMR spectrum being featureless, we ran mass spectroscopy analyses and could obtain a signal corresponding to the monomeric form $[L_2^*FeCl]^{+}$, L_2^* being the O-demethylated form of L_2 . Ferric mononuclear complexes of similar structure exist: we reported in the past the structure of an analogue compound in which the iron center is bound to a catechol moiety.¹⁸ In the present case, however, the elemental analysis was in contradiction with the occurrence of a mononuclear structure. The results strongly suggested that the observed $[L_2^*FeCl]^{+}$ in mass spectrometry was the result of a fragmentation. Indeed, the elemental analysis data supported the presence of a dinuclear asymmetric complex (one ligand for two metals), as it is generally the case for oxygenation products with sterically hindered ligands.^{16,17} Additionally, the fact that around 50% of the total ligand was released as a free tripod upon oxygenation also brought credit to the presence of an asymmetric complex.

We found in the past that using simple redox reactions can lead to indirect characterization of complexes.¹⁸ At this point, we examined the cyclic voltammetry data of the green compound, exhibiting two waves at low and moderate negative potentials, the first being fully reversible. With hope that the structure would not be considerably modified upon full reduction (the reduction potential of Zn/Hg lies far below the second irreversible reduction wave of our complex³³), we reacted the dark green compound with zinc amalgam. This quickly afforded a bright orange complex with an excellent yield, which was revealed to be extremely sensitive to dioxygen. Its UV spectrum strongly suggested the presence of a phenolate coordinated to a ferrous center.¹⁸ The evidence for one O-demethylation of the ligand came from examination of the crystal structure, which also confirmed the presence of an asymmetric dinuclear species. The two-step transformation of L_2FeCl_2 into $L_2^*FeCl_3$ is displayed in Scheme 2.

We recently showed that, upon reduction with Zn/Hg, μ -oxo di-ferric complexes convert back to the ferrous mononuclear complexes.¹⁷ Thus, if any μ -oxo (or μ -hydroxo) bridge was present in the dark green compound, it would probably have been removed upon reduction. This is the reason why we cannot directly extrapolate the structure of $L_2^*Fe_2Cl_3$ to describe that of the green precursor. However, on the basis of analytical and

spectroscopic methods, and keeping in mind the sensitivity of the compound toward bases, it seems that the structure $[L_2^*Fe-OH-FeCl_3]Cl$ represents the most likely hypothesis. The unquestionable point remains that O-demethylation of the ligand has occurred upon the reaction of dioxygen with the metal center in L_2FeCl_2 .

In the chemistry of cytochromes P-450, O-demethylation is proposed to occur via reaction of the methoxy group with the oxygen-active species (a formal Fe(V)=O center, in fact an Fe(IV)=O/protein radical transient²⁹), although the way demethylation occurs is not known yet.⁸⁻¹⁴ In the present case, oxygenated species (an *oxy* form such as Fe(II)O₂, and perhaps an *oxo* form such as Fe(IV)=O) of iron complexes have to be present in the medium.^{15,17} If one considers the regiospecificity of the reaction, that is, the fact that only the ortho OMe group of the substituent is O-demethylated, the occurrence of a process involving radical scrambling in solution seems very unlikely. By contrast, the presence of the chloride-methoxy interaction in the crystal structure of L_3FeCl_2 validates the hypothesis of an interaction between the methoxy group and any oxygenated form of the metal center. In the present case, the oxygen-adduct $Fe^{II}(O_2) \leftrightarrow Fe^{III}-O-O\cdot$ might promote hydroxylation of the adjacent methoxy group with a release of formaldehyde and concomitant formation of an $Fe^{IV}=O$ species. Upon reaction with the starting complex, this high-valent species would form an asymmetric $Fe^{III}-O-Fe^{III}$ with a pendant phenol arm, and there would be a release of the free unmodified ligand. Subsequent rearrangement would yield a $Fe^{III}(PhO)(OH)Fe^{III}$ asymmetric complex with phenolato and hydroxo bridging ligands.

Why such a reaction with L_2FeCl_2 and not L_1FeCl_2 , for which the formation of a standard μ -oxo species is observed? It seems likely that, in the case of L_2FeCl_2 , at least one substituted pyridine remains coordinated during the oxygenation process, forcing the methoxy group to lie in close proximity to the active metal center. This is actually a prerequisite for the reaction to occur. This is not necessarily the case with a single-substituted ligand in which some flexibility might lead to temporary decoordination of the more bulky substituted arm.²⁰ Again, this finding supports a metal-centered process rather than a free radical-based reaction.

Concluding Remarks

The formation of μ -oxo diferric complexes from molecular dioxygen and mononuclear Fe(II) complexes is currently

(33) Bard, A. J.; Faulkner, L. R. In *Electrochemical Methods. Fundamentals and Applications*; John Wiley and Sons, Inc. Publishers: New York, 1980.

emerging as a general process within nonporphyrinic chemistry.^{16,17,34–36} Kinetic and electrochemical studies strongly support the formation of some dioxygen–metal adduct, although the structure of such a species at a single metal site has never been reported in nonporphyrinic chemistry.^{3,17,34,37,38} There are a few reports of intramolecular transformations of a ligand upon oxygenation (rearrangements, N-dealkylation, oxidative dehydrogenation, or intramolecular hydroxylations to cite a few examples^{39–45}); however, O-demethylation is in general poorly mentioned, and when it is, it is as a side and nondesirable reaction.^{11,12}

The present study brings to light two particular comments.

The first message of the present work is to demonstrate that, even when the geometry at the metal site seems extremely favorable to dioxygen coordination, the process is controlled by electronic and structural factors: thus, a

16-electron complex with a five-coordinate environment might turn out to react slowly (L_2FeCl_2) or very poorly (L_3FeCl_2).

The second outcome is the occurrence of a regiospecific intramolecular O-demethylation of the ligand that occurs when methoxy groups are kept in place, close to the metal center. This is one of the first examples known in homogeneous nonheme chemistry, which parallels a well-known reaction in P-450 chemistry. Does it mean that an oxo-ferryl $Fe=O$ moiety with strong oxidation abilities is formed upon oxygenation of our complex? Although unlikely, we cannot rule out this hypothesis. Or inversely does it mean that, even in the case of the P-450s, O-demethylation of substrates—kept in place at the distal side before the oxygenation—does not necessarily need the presence of a high-valent oxo-ferryl $Fe=O$ center but simply an oxygenated form (whatever its nature may be) of the metal center? Even if we tend to favor this hypothesis in the present case, the question remains open. In any event, experimental evidence leads to the conclusion that coordination of dioxygen close to a judiciously oriented methoxy group is a minimum requirement.

Acknowledgment. This work was supported as a collaborative action between CNRS (project no. 18552—France) and CNRST (project no. chimie 08/06 and 08/07—Morocco). Both organizations are gratefully acknowledged for their support. We also wish to thank Dr. Remy Louis, head of the Institut de Chimie in Strasbourg, for constant support and encouragement, and the CNRS and ULP. The Conseil Scientifique de l'ULP is acknowledged for specific support, no. AO CS ULP 2006.

Supporting Information Available: All synthetic details including the preparation and characterization of all compounds mentioned. For the four reported structures, the crystallographic files in CIF format have been deposited. This material is available free of charge via the internet at <http://pubs.acs.org>.

(34) Korendovych, I. V.; Kryatova, O. P.; Reiff, W. M.; Rybak-Akimova, E. V. *Inorg. Chem.* **2007**, *46*, 4197–4211.

(35) Zart, M. K.; Powell, D.; Borovik, A. S. *Inorg. Chim. Acta* **2007**, *360*, 2397–2402.

(36) Dutta, S. K.; Ghosh, M.; Biswas, P.; Flörke, U.; Saal, C.; Haase, X. X.; Nag, K. *New J. Chem.* **2007**, *31*, 93–101.

(37) Carvalho, N. M. F.; Antunes, O. A. C.; Horn, A. Jr. *Dalton Trans.* **2007**, 1023–1027.

(38) May, Z.; Simandi, L. I.; Vertes, A. J. *Mol. Catal. A* **2007**, *266*, 239–248.

(39) Nehru, K.; Seo, M. S.; Kim, J.; Nam, W. *Inorg. Chem.* **2007**, *46*, 293–298.

(40) Celenligil-Cetin, R.; Paraskevopoulou, P.; Dinda, R.; Staples, R. J.; Sinn, E.; Rath, N. P.; Stavropoulos, P. *Inorg. Chem.* **2008**, *47*, 1165–1172.

(41) Celenligil-Cetin, R.; Paraskevopoulou, P.; Dinda, R.; Lalioti, N.; Sanakis, Y.; Rawashdeh, A. M.; Staples, R. J.; Sinn, E.; Stavropoulos, P. *Eur. J. Inorg. Chem.* **2008**, 673–677.

(42) Machkour, A.; Mandon, D.; Lachkar, M.; Welter, R. *Eur. J. Inorg. Chem.* **2005**, 158–161.

(43) Menage, S.; Galey, J. B.; Dumats, J.; Hussler, G.; Seite, M.; Gautier-Luneau, I.; Chottard, G.; Fontecave, M. *J. Am. Chem. Soc.* **1998**, *120*, 13370–13382.

(44) Lange, S. J.; Miyake, H.; Que, L. Jr. *J. Am. Chem. Soc.* **1999**, *121*, 6330–6331.

(45) Yamashita, M.; Furutachi, H.; Tosha, T.; Fujinami, S.; Saito, W.; Maeda, Y.; Takahashi, K.; Tanaka, K.; Kitagawa, T.; Suzuki, M. *J. Am. Chem. Soc.* **2007**, *129*, 2–3.